
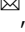




Caves demonstrate decrease in rainfall recharge of southwest Australian groundwater is unprecedented for the last 800 years

Stacey C. Priestley ^{1,2,6}, Pauline C. Treble^{1,3}, Alan D. Griffiths¹, Andy Baker ³, Nerilie J. Abram ^{4,5} & Karina T. Meredith^{1,3}

Billions of people worldwide rely on groundwater. As rainfall in many regions in the future is projected to decrease, it is critical to understand the impacts of climate change on groundwater recharge. The groundwater recharge response to a sustained decrease in rainfall across southwest Australia that began in the late 1960s was examined in seven modern speleothems and drip waters from four caves. These show a pronounced increase or uptick in regional drip water and speleothem oxygen isotopic composition ($\delta^{18}\text{O}$) that is not driven by a change in rainfall $\delta^{18}\text{O}$ values, but is in response to the shallow karst aquifers becoming disconnected from rainfall recharge due to regional drying. Our findings imply that rainfall recharge to groundwater may no longer be reliably occurring in this region, which is highly dependent on groundwater resources. Examination of the longer speleothem record shows that this situation is unprecedented over the last 800 years.

¹ANSTO, Lucas Heights, NSW, Australia. ²School of Physics, Chemistry and Earth Sciences, The University of Adelaide, Adelaide, SA, Australia. ³School of Biological, Earth and Environmental Sciences, UNSW Sydney, Sydney, NSW, Australia. ⁴Research School of Earth Sciences, Australian National University, Canberra, ACT, Australia. ⁵ARC Centre of Excellence for Climate Extremes, Australian National University, Canberra, ACT, Australia. ⁶Present address: CSIRO Environment, Glen Osmond, SA, Australia. email: stacey.priestley@csiro.au

Groundwater use is accelerating globally due to population growth^{1,2}. Further reductions in water availability in many regions due to climate change^{3,4} are likely placing increasing pressure on groundwater resources and groundwater-dependent ecosystems^{5,6}. It is critical to understand how drying in the mid-latitudes will impact rainfall recharge to groundwater resources globally, yet our current understanding of the sensitivity of groundwater systems to climate change is limited^{4,7–9}. This is because water table monitoring using direct methods such as bores can be complicated by groundwater extraction and land use change which can obscure the climate change signal¹⁰, and the water table may be recharged by rivers or lakes¹¹ in addition to local rainfall recharge. Furthermore, the hydraulic memory of groundwater systems can delay a response to climate change by decades or longer¹. These factors mean that attributing changes in groundwater recharge to the impacts of climate change on rainfall and the surface water balance is difficult.

Caves offer a natural window to observe the movement of water from the surface through the vadose zone and into groundwater aquifers, and can thus indicate rainfall recharge to groundwater^{12,13}. Rainfall recharge may be via preferential flow along fractures, fracture and fissure zones and conduits, or it can be diffuse porous flow through the matrix. In karst environments, recharge is likely to be a mixture of diffuse and preferential-flow types^{12,14}. Similar to groundwater, the oxygen isotopic composition ($\delta^{18}\text{O}$) of cave drip waters and consequently speleothems, is largely determined by the recharge-weighted $\delta^{18}\text{O}$, particularly in water-limited climates^{15,16} where groundwater resources are increasingly under pressure. Accordingly, speleothems offer a highly temporally-resolved record of rainfall recharge to groundwater. As speleothems form in the vadose zone above the water table, they are not complicated by modern groundwater abstraction nor the longer-term processes such as changes in hydraulic boundary conditions. Modern speleothems formed since the early 20th century can be used to assess the response of rainfall recharge to groundwater during recently observed climate change, while older speleothem material can provide a longer-term context of the range of natural, pre-industrial variability of rainfall recharge to groundwater.

Rainfall in southwest Australia is highly seasonal and falls in the cooler months, typically from May to October. The southwest Australian region has experienced a prolonged decline in annual rainfall (Fig. 1) attributed to changes in Southern Hemisphere atmospheric circulation systems with a considerable contribution from anthropogenic forcing^{17,18}. In response to anthropogenic changes in stratospheric ozone and then atmospheric greenhouse gases¹⁸, rainfall has decreased by 10–25% overall across the region since the 1960s¹⁹. This has resulted in an annual rainfall decrease of between 100 and 230 mm since 1971–2010 compared to 1911–1970 (Fig. 1). Several local studies have since recognised the effect of reduced rainfall and increased abstraction on water resources within southwest Australia, as direct rainfall recharge has generally been found to be the major recharge mechanism^{20,21}. For example, the Rottnest Island freshwater lens (Fig. 1) has decreased in size by 40% primarily due to the rainfall decrease²⁰. Likewise, water table decline within the Perth Basin has been identified as a result of decreasing rainfall^{21,22}. However, quantifying the amount of water table decline attributable to decreased rainfall input is complicated by increasing groundwater extraction and land use changes over the same time period²³. Climate models indicate, with high confidence, that rainfall in this region is likely to decline further throughout the 21st century¹⁸ which will continue to impact water availability in southwest Australia^{21,22}. This will have a consequent impact on water-dependent ecosystems²⁴ and water security for this region that currently depends on groundwater to meet 75% of its water demand²¹.

In this study, we constructed a composite speleothem $\delta^{18}\text{O}$ record using seven speleothems from four caves across a 30-km transect in southwest Australia (Fig. 1; see Supplementary Fig. 1 for speleothem images). All caves are located in the Leeuwin-Naturaliste National Park and are developed in the Late Quaternary aeolian calcarenite that outcrops along the coast²⁵. All caves are located in the vadose zone and receive recharge from rainfall only. No surface runoff is observed at the caves due to the free-draining quartz-rich sandy soil with infiltration also aided by seasonal rainfall occurring in the cooler months. See Table 1 for a summary of climate, vegetation and cave sampling locations.

One of the caves, Golgotha Cave, has been extensively monitored between 2005 and 2020 including for stable isotopes of rainwater²⁶ and cave drip water from the locations of four speleothems presented here²⁷. Opportunistic campaign sampling of ~20 additional drip sites in Golgotha Cave occurred during five field campaigns conducted in 2012, 2013 and 2014 (see Supplementary Table 1)²⁷. The flow classification of these drips was determined in refs. 12,28,29 using statistical analysis of stalactites mapped by lidar and automated drip rate loggers. Recent studies identified that rainfall recharge through Golgotha Cave occurs via drips that are a mixture of slow diffuse flow, predominantly through the matrix, and faster preferential flow focussed along fractures or conduits²⁷. For brevity, we refer to these henceforth as diffuse versus preferential-flow paths. Deep percolation via rapid movement of water along preferential flow paths is supported by threshold increases in drip rates¹² and water oxygen isotope studies²⁷. See Supplementary Note 1 for detailed site descriptions.

The stalagmites used in this study have all grown through the period of recent regional rainfall decline (Fig. 1). The speleothem $\delta^{18}\text{O}$ records, along with cave drip water monitoring, demonstrate a common rise, or uptick, in values beginning in the 1990s. The uptick is not driven by a change in the input source water (rainfall) $\delta^{18}\text{O}$ values but rather is demonstrated to be a shift in the hydraulic flow properties in the karst aquifer in response to reduced rainfall recharge. We argue that the declining rainfall has reduced rainfall recharge to groundwater along preferential-flow paths. We also assess this in the context of the longer (paleo) speleothem record for the region and demonstrate that this uptick is unprecedented for the last 800 years, implying that the current reduction in rainfall recharge is also unprecedented over this period.

This study uses seven modern speleothems, as well as cave drip water, from multiple caves to examine the response of reduced rainfall recharge due to climate change in the modern record. In doing so, it also confirms that upticks in speleothem $\delta^{18}\text{O}$ values primarily represent reduced water supply to the speleothem. This substantiates the interpretation of speleothem $\delta^{18}\text{O}$ datasets as a proxy for hydroclimate, and importantly validates the role of karst flow paths in driving a non-linear response to hydroclimate forcing via control on recharging water $\delta^{18}\text{O}$ values.

Results and discussion

Composite speleothem $\delta^{18}\text{O}$ record. Seven speleothem records from four caves, as well as cave drip water $\delta^{18}\text{O}$ data from one of the caves (Fig. 2), were used to construct a composite speleothem $\delta^{18}\text{O}$ record (Fig. 3a). These records all demonstrate a rise or uptick in $\delta^{18}\text{O}$ values during the late 20th Century and early 21st Century. The rising trend in the Golgotha Cave speleothem and drip water $\delta^{18}\text{O}$ values in recent decades was first reported in ref. 27 and is now replicated here in additional speleothems from other caves in the Cape Leeuwin-Cape Naturaliste region. The rise in $\delta^{18}\text{O}$ for speleothem MND-S1 in response to the first rainfall decrease was initially documented in ref. 30, although this

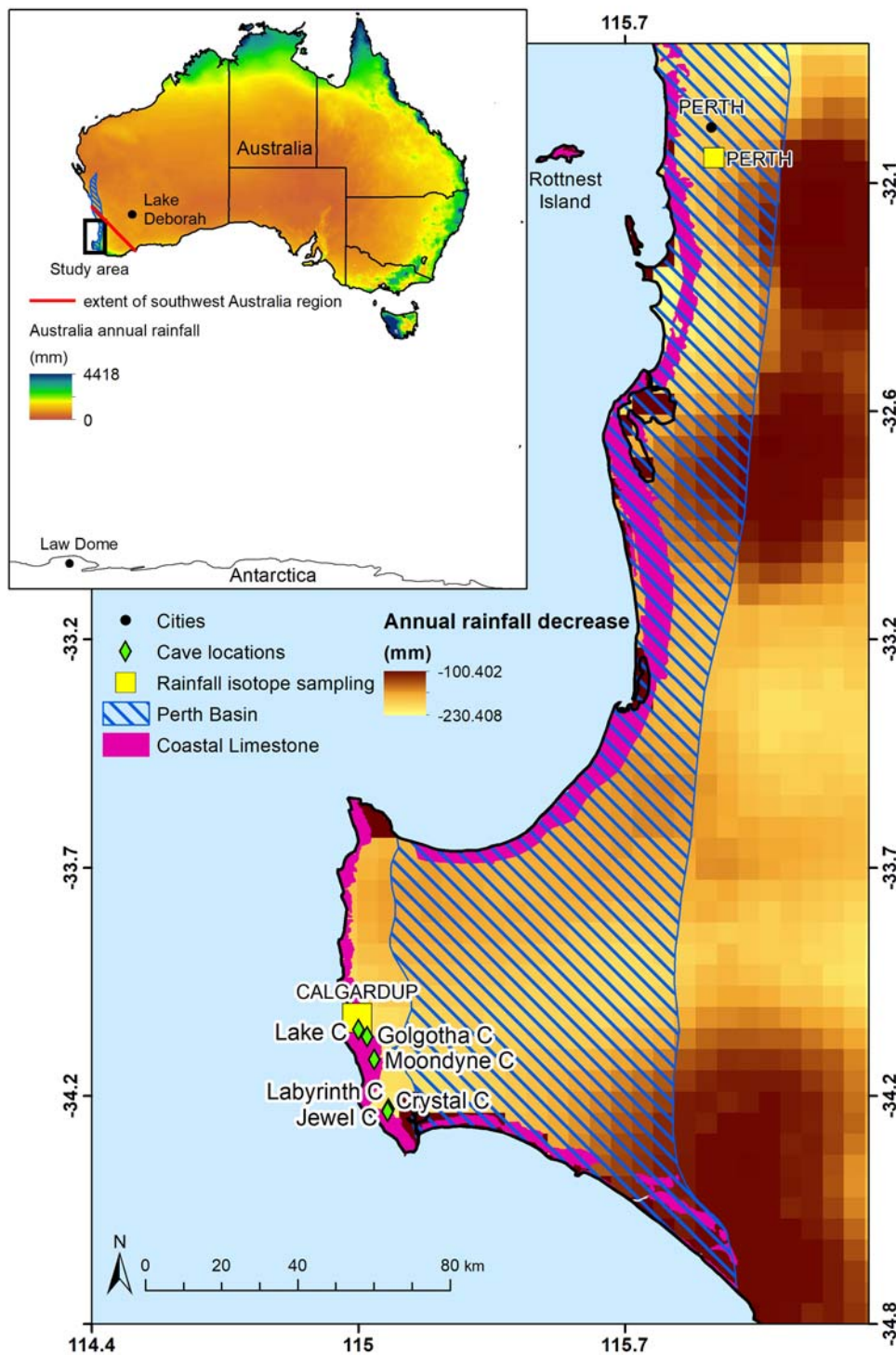


Fig. 1 Location of caves and regional rainfall decrease. The map shows the location of caves, rainfall samples and the total decrease in annual rainfall for 1971–2010 compared to 1911–1970³³. See Supplementary Note 1 for description of field sites and stalagmite samples. Inset shows the study area location, full extent of groundwater in the Perth Basin (hatched area) and extent of southwest Australian region (shown by red line joining 30°S, 115°E and 35°S, 120°E). Annual rainfall shown on the inset map shows that the study area is in an important rainfall area of the southern Australian region.

record ceased in 1992 when the speleothem was removed, i.e., too early to record the full extent of the $\delta^{18}\text{O}$ uptick. New data presented in this study from speleothems, CRY-S1 and LAB-S1, as well as GL-S4 from ref. ²⁷, cover a longer period since the rainfall decrease (CRY-S1 and LAB-S1 ceased in 2009 CE while GL-S4 in 2012 CE; Fig. 2). These three records replicate the rising isotopic trend recorded in the drip water monitoring during the respective periods of overlap with the monitoring data (Fig. 2),

confirming the robustness of the uptick as a regional signal (Fig. 3a). The beginning of the uptick varies between speleothem records which may be due to different hydraulic response times (i.e., cave flow properties) or speleothem age uncertainty, although the latter is small (see Methods). Nevertheless, the comparison of records indicates that the isotopic rise becomes a common signal by the 1990s. The speleothem records show that this rise is approximately 1‰, while our drip water data confirm

Table 1 Summary of speleothem sites and sample information.

Sample code	Site information			Sample information		Climate statistics			Source previously published data		
	Name	Lat (°S), Lon (°E)	Altitude (m ASL)	Soil thickness (m)	Limestone thickness (m)	Cave T (°C)	Distance from entrance (m)	MAT (°C)		Rainfall (mm)	Actual evapotranspiration (mm)
CRY-S1	Crystal C.	34.1, 115.0	100	Unknown, likely similar to Golgotha C.	40	Unknown	140	15.6 ± 0.5	1101 ± 157	730 ± 42	Chronology ⁴⁹ δ ¹⁸ O, this study Chronology ²⁷ δ ¹⁸ O
GL-S1, GL-S2, GL-S3, GL-S4	Golgotha C.	34.1, 115.1	70	Variable 0.3 – 3 m	30 (GL-S1, GL-S4) 40 (GL-S2, GL-S3)	14.5–14.8	60 (GL-S1, GL-S4) 90 (GL-S2, GL-S3)	15.6 ± 0.5	1101 ± 157	730 ± 42	
LAB-S1	Labyrinth C.	34.3, 115.1	65	Unknown, likely variable as for Golgotha C.	35	15.9–16.5	unknown	16.6 ± 0.4	1095 ± 164	609 ± 47	Chronology ⁵¹ δ ¹⁸ O, this study Chronology ³⁰ δ ¹⁸ O ³⁰
MND-S1	Moondyne C.	34.3, 115.1	65	Unknown, likely variable as for Golgotha C.	15–20	15.9–16.5 ⁵⁰	60	16.6 ± 0.4	1095 ± 164	609 ± 47	

Locations are rounded to the nearest tenth of a degree, as exact locations are not disclosed for cave conservation purposes. Soil thickness is approximate from field observations. All caves are located within 8 km from Australian Bureau of Meteorology stations and climate statistics are calculated over the period 1911–2020 from data extracted for the sites from the AWRRA-L dataset⁴⁶. All caves are located in *Eucalyptus* forest with dense understorey and are located in Leeuwin-Naturaliste National Park.

that this rising trend has continued to the present, indicating an overall increase of 1.5‰ above the 1900–1968 normalised speleothem δ¹⁸O baseline (Fig. 3a).

Speleothem δ¹⁸O is a function of multiple processes^{31,32}, and can be altered due to changes in water–calcite reaction processes such as: (1) cave temperature, (2) isotopic disequilibrium and/or (3) kinetic fractionation due to precipitation rate; as well as a function of drip water isotopic composition. However, as shown below, neither changes in cave temperature nor other changes in reaction processes can account for the observed uptick.

The uptick in speleothem δ¹⁸O cannot be attributed to the temperature-dependent fractionation that occurs during calcite precipitation³¹ as recent warming³³ would lower speleothem δ¹⁸O by an estimated 0.27‰ below pre-1960 values rather than raise speleothem δ¹⁸O values as observed (Fig. 3a). Enhanced isotopic disequilibrium processes^{31,34} (disturbance of the isotopic equilibrium between H₂O and the carbonate species) were shown not to be dominating δ¹⁸O variability in the modern Golgotha Cave records, representing four of the seven stalagmites in our composite²⁷. This was constrained numerically by demonstrating that the O isotopic fractionation factors (α_{calcite-water}) were spatially consistent across the four sites and temporally consistent over the period of rising drip water δ¹⁸O values (see ref. ²⁷ their Table 2 and their Supplementary Note 2). Moreover, cave temperature has been monitored at the same site in Golgotha Cave in discontinuous intervals since 2005 and has not risen (see Supplementary Table 2). We further tested for changes in precipitation rate, which may drive the isotope fractionation factor further from predicted (kinetic isotope fractionation³⁵), by calculating annual extension rate using laminae width for the three speleothem records with the longest datasets (CRY-S1, LAB-S1 and GL-S4) and the pre-uptick versus uptick mean annual extension rates were within ± 1 standard deviation, indicating that this is not the driver of the uptick. Hence water–calcite reaction processes do not account for the magnitude of the uptick and, furthermore, could not have produced the rising trend observed in the drip water δ¹⁸O values.

The observed uptick is present in both the drip water and speleothem δ¹⁸O values. The rising trend in the Golgotha Cave speleothem and drip water δ¹⁸O values in recent decades was first reported in ref. ²⁷ and is now replicated here in additional speleothems from other caves in the region. This implies a regionally consistent response of drip water δ¹⁸O to hydrological forcing persisting over several decades, and is examined further below.

Rainfall recharge and the drip water δ¹⁸O response

Southwest Australian rainfall δ¹⁸O. Long-term changes in mean rainfall δ¹⁸O values have the potential to drive similar changes in drip water δ¹⁸O values³¹. Rainfall δ¹⁸O and its relationship to climate in southwest Australia has been previously studied²⁶, and these datasets can help constrain the impact of climate change on rainfall δ¹⁸O in the region²⁶. The decline in southwest Australian winter rainfall has occurred in two steps occurring in 1968/1969 and 1999/2000¹⁹ (Fig. 3b). This regional pattern of rainfall decline (Fig. 1) is also evident over the narrow coastal limestone belt where the caves are located (Fig. 3b). The rainfall decrease has been characterised as a reduction in total rainfall and heavy rainfall during winter, as well as a decrease in the total number of rain days³⁶. Of these three factors, it is rainfall intensity that most impacts the δ¹⁸O value of southwest Australian rainfall (see ref. ²⁶ which shows that more intense rainfall is associated with more negative δ¹⁸O values). However, using both measured and modelled rainfall δ¹⁸O values (Fig. 3c), we can quantify that the observed change in rainfall intensity accounts for between

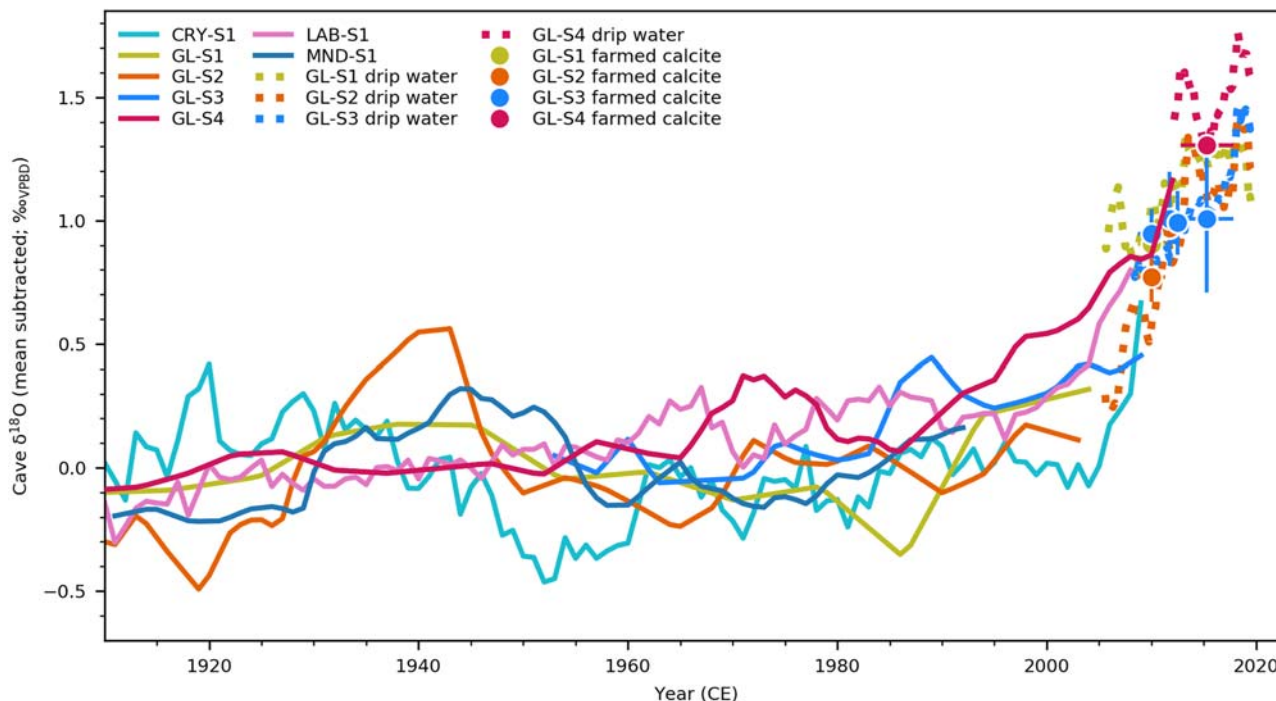


Fig. 2 Modern speleothem and drip water records. Individual speleothem (stalagmite) $\delta^{18}\text{O}$ records from Crystal Cave (CRY-S1), Golgotha Cave (GL-S1, GL-S2, GL-S3 and GL-S4), Labyrinth Cave (LAB-S1), and Moondyne Cave (MND-S1), as well as drip water $\delta^{18}\text{O}$ expressed as calcite-equivalent values and farmed calcite $\delta^{18}\text{O}$ from the Golgotha speleothem locations. Farmed calcite $\delta^{18}\text{O}$ error bars represent ± 1 standard deviation of measurements from each site and the year error bars represent the sample collection time. All data were normalised by subtracting 1900–1968 mean speleothem $\delta^{18}\text{O}$ values. Chronologies for all speleothems were published previously (see 'Methods').

a -0.3‰ to $+0.1\text{‰}$ change in precipitation-weighted mean annual rainfall $\delta^{18}\text{O}$ values over the period of rainfall decline (Table 2). In contrast, the measured rise in the composite $\delta^{18}\text{O}$ record of 1.5‰ is fifteen times greater (Fig. 3a). Thus, we argue that the overall rise of 1.5‰ in our composite $\delta^{18}\text{O}$ record reflects a rise in drip water $\delta^{18}\text{O}$ despite little change in the mean $\delta^{18}\text{O}$ value of annual rainfall supplying these drips.

Considering that temporal variability in mean rainfall $\delta^{18}\text{O}$ values cannot account for the observed rise in drip water $\delta^{18}\text{O}$, the possible remaining processes are (1) isotopic modification of the infiltrated rainwater by rising evapotranspiration demand, (2) increasing evaporation of soil water from within karst flow paths³⁷ and/or (3) a shift in the dominant flow paths supplying drip water to a stalagmite, i.e., a change in the contribution of diffuse versus preferential flow²⁷. These remaining processes are discussed below.

Evapotranspiration and soil/karst evaporation. Evapotranspiration demand is potentially important in this environment as evapotranspiration fluxes for Golgotha Cave are high due to water demand from the overlying forest, and the soil profile becomes dry during the warmer months^{38,39}. Transpiration does not result in isotopic fractionation of soil water⁴⁰ although it is plausible that transpiration could alter the fraction of rain events contributing to drip water, but this should favour the removal of smaller rain events (relatively higher $\delta^{18}\text{O}$ values)²⁶ during the dry summer months when vegetation water stress is highest. Thus, an increase in transpiration demand is likely to lower, rather than raise, the mean value of rainfall recharge $\delta^{18}\text{O}$, i.e., opposite to the observed change. Hence we rule out this process as the driver of the uptick.

To diagnose the effect of evaporation in the soil, Fig. 4 shows isotopic composition of rainfall and flow-classified campaign drip water data on a δD versus $\delta^{18}\text{O}$ plot. Linear fits to each category:

rainfall (also known as the local meteoric water line or LMWL), diffuse flow and preferential flow; have slopes which are indistinguishable when judged from the 95% confidence interval, although the slope for diffuse-flow drips appears to have a lower value than other categories (Fig. 4, inset). This indicates the possible incorporation of a small fraction of water affected by evaporation in the soil zone, preferentially into the diffuse-flow path (cf. ref. ³⁷). For example, soil zone evaporation at Golgotha Cave was proposed by ref. ³⁸ to explain a transient peak whereby drip water $\delta^{18}\text{O}$ values rose 2.5‰ and returned to long-term mean values within 12 weeks. However, it was observed that the contribution of isotopically-modified soil water was small and was quickly diluted by the newly infiltrated water in the following recharge season. Thus soil water evaporation is a process which can affect drip water, at least transiently, but since it is short-lived and not affecting preferential flow $\delta^{18}\text{O}$ values (Fig. 4, inset), it is unlikely to contribute enough volumetrically to drive the uptick in observed $\delta^{18}\text{O}$ values. The overall similarity of the slope of values of the drip waters to the LMWL supports our interpretation that evaporation under low humidity (the soil zone) has not substantially modified the drip waters.

If evaporation in the soil zone is unlikely to drive the uptick, there is also the potential for the diffusional loss of water vapour from the deeper karst zone to dry the deep water stores and concurrently affect drip water isotopes. For this process, the δD versus $\delta^{18}\text{O}$ slope values are not a helpful diagnostic as we can assume that liquid water below the surface is in equilibrium with the surrounding vapour, hence relative humidity is close to 100% and isotopic fractionation is governed by equilibrium processes so that isotopic values evolve along the same line as the LMWL (see ref. ³⁷ for further discussion). The relative magnitude of this process on the drip water $\delta^{18}\text{O}$ values may also be estimated by comparing the calculated drip $\delta^{18}\text{O}$ using the regression relationships on Fig. 4 for preferential versus diffuse flow, and

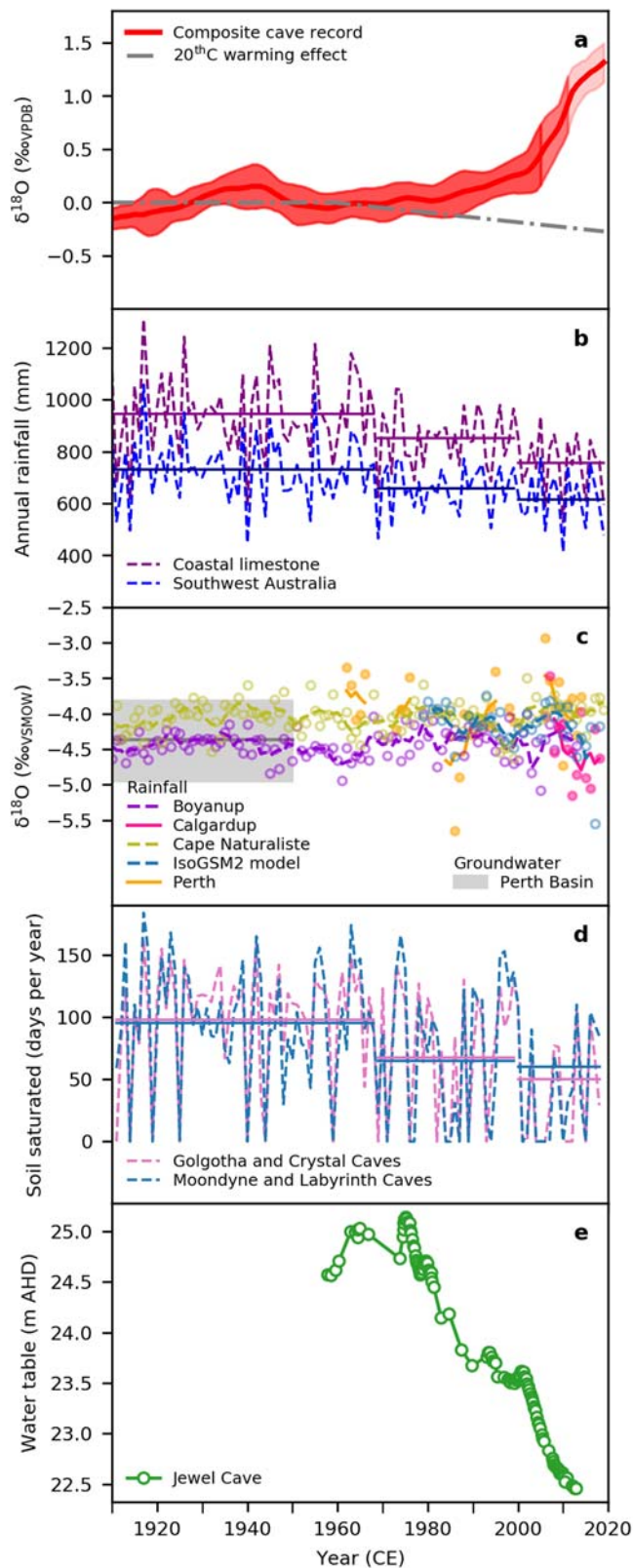


Fig. 3 The uptick in cave $\delta^{18}\text{O}$ data is too large to be driven by changes in mean annual rainfall $\delta^{18}\text{O}$ and is interpreted to be a reduction in preferential flow reaching the cave. **a** Composite cave $\delta^{18}\text{O}$ record that is the 5-year rolling average of the 1900–1968 mean subtracted speleothem and drip water records. Shaded area represents one standard deviation. Calculated 20thC warming effect on $\delta^{18}\text{O}$ values also shown. **b** Rainfall amount for the southwest Australian region (southwest of the line joining 30°S, 115°E and 35°S, 120°E; Fig. 1, inset) and for the coastal limestone extent (Fig. 1) demonstrating that the coastal locations of the caves also experienced two decreases in regional rainfall. Means for the periods 1910–1968, 1969–1999, and 2000–2020 are represented by horizontal lines. **c** Five-year rolling averages of annual amount-weighted rainfall $\delta^{18}\text{O}$: measured at Calgardup and Perth; predicted from high quality long-term rainfall records at Boyanup and Cape Naturaliste; and predicted from IsoGSM2⁵⁷. Circles of the same colour correspond to the monthly amount-weighted rainfall $\delta^{18}\text{O}$. Also, range of $\delta^{18}\text{O}$ measured in groundwater from the Leederville and Yarragadee aquifers of the Central and Southern Perth Basin⁵⁸. **d** Number of days per year soil is saturated with horizontal bars indicating the average values across all of the cave sites for the periods 1910–1968, 1969–1999 and 2000–2020. Three model estimates were determined corresponding to the three 0.05° gridded cells covering the four cave sites in the AWRA-L model⁵⁶. **e** Local water table level beneath Jewel Cave.

the flow paths by preferential flow over time could increase the potential for evaporation under high humidity of slower percolating diffuse-flow water, and this is consistent with our interpretation outlined below that there has been a reduction in the preferential flow component owing to the decline in rainfall.

Flow paths supplying drip water. In the study of Golgotha Cave drip waters by ref. 27, it was shown that drip water influenced by preferential flow typically has lower $\delta^{18}\text{O}$ values compared with drip water predominately supplied by diffuse flow. Figure 5 shows the distributions of drip water compared with rainwater $\delta^{18}\text{O}$ values for these data. Based on the campaign data, which sampled the largest number of drip locations, the distribution mode of diffuse-flow dominated drips ($-4.12 \pm 0.12\text{‰VSMOW}$) is closest to the precipitation-weighted mean of rainfall ($-3.61 \pm 0.21\text{‰VSMOW}$), whereas the distribution mode of preferential-flow-influenced drips ($-4.67 \pm 0.06\text{‰VSMOW}$) are 1‰ lower than rainfall (Fig. 5). The lower value for the preferential flow $\delta^{18}\text{O}$ values is closer to rainfall when only heavier totals are included ($-4.55 \pm 0.40\text{‰VSMOW}$, daily events >9 mm; Fig. 5). Drip water $\delta^{18}\text{O}$ values lower than rainwater is characteristic of the typical recharge-bias response seen at a global scale in cave drips^{15,27}. The isotopic distinction in drip flow type is also evident in two of the speleothem drip sites classified as predominately diffuse (GL-S1, mode = $-3.99 \pm 0.03\text{‰VSMOW}$) and preferential flow influenced (GL-S3, mode = $-4.60 \pm 0.04\text{‰VSMOW}$). We note here that the distribution of the diffuse-dominated drip waters appears bimodal, indicating that the majority of drips are a mixture of diffuse and preferential flow with the contributions of preferential flow varying over time due to the higher recharge threshold required to activate flow along the fractures. See ref. 27 for an example of flow activated along a fracture after high recharge, captured in the drip time series for speleothem GL-S4, that led to a 0.5‰ decline in drip water $\delta^{18}\text{O}$ values.

Each speleothem in our composite record will have unique flow path properties and length, yet as with the drip water, all are likely influenced by a mixture of diffuse plus additional preferential flow. Fewer of these preferential-flow recharge events, resulting in a drift towards the higher isotopic value of the diffuse-flow dominated drips, is the most likely explanation for the 1–1.5‰ uptick in drip water and speleothem $\delta^{18}\text{O}$. We further interpret

can be shown to be small. For example, using the precipitation-weighted δD mean value of rainfall (-20.2‰ ; ref. 26), the estimated increase in drip $\delta^{18}\text{O}$ is 0.1‰ due to evaporation at high humidity. Thus, while this process may always be present, it also appears to be insufficient in magnitude to be responsible for the uptick. Nonetheless, we propose that less frequent recharge of

Table 2 A comparison of precipitation-weighted annual rainfall mean $\delta^{18}\text{O}$ values before and after southwest Australian rainfall decreased.

Dataset	Measured and modelled mean annual rainfall $\delta^{18}\text{O}$ values (‰)		
	1908–1968	1969–2018	Difference
Perth measured ⁵⁴	-3.70 ± 0.07 (1962–1966)	-4.02 ± 0.02 (1973–1976, 1984–1995, 1998–2000, 2005–2014)	-0.32
Calgardup measured ²⁶	-	-4.44 ± 0.14 (2006–2018)	-
Boyanup simulated ²⁶	-4.47 ± 0.02	-4.38 ± 0.03 (1969–2013)	+0.09
Cape Naturaliste simulated ²⁶	-4.05 ± 0.03	-4.04 ± 0.03	-0.01
IsoGSM ⁵⁷	-	-4.18 ± 0.05 (1979–2018)	-

1968/1969 was used for the timing of the decrease following the analysis of ref. 19.

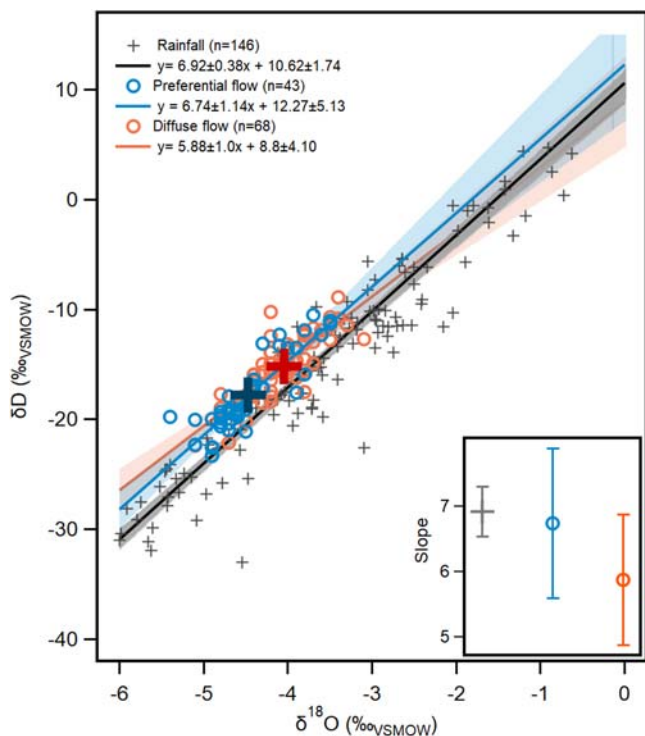


Fig. 4 Water isotope plot comparing drip water and local rainfall. Rainfall data are from ref. 26, and drip water are from the five sampling campaigns described in the text. The regression, or local meteoric water line (LMWL), was calculated using the precipitation-weighted method (WLS-LMWL) in ref. 26. Confidence interval is 95%. Large crosses are the distribution modes for preferential flow (blue; $\delta^{18}\text{O} = -4.67 \pm 0.06\text{‰}$, $\delta\text{D} = -19.32 \pm 1.21\text{‰}$) and diffuse flow (orange; $\delta^{18}\text{O} = -4.12 \pm 0.12\text{‰}$, $\delta\text{D} = -15.09 \pm 0.79\text{‰}$). Inset compares slope values and error bars represent ± 2 standard error. The similarity of the slope values of the drip waters and local rainfall suggests that evaporation under low humidity (soil zone) has not substantially modified the drip waters.

that the reduction in this preferential-flow component is due to the rainfall decrease that this region has experienced (Fig. 3b), owing to the impact on soil moisture balance which we outline below.

Movement of water along preferential-flow paths requires overlying soils to have become saturated⁴¹, consistent with observations at Golgotha Cave³⁹. In a time-lapse electrical resistivity tomography study, it was observed that autumn and early winter rains saturate the soil and epikarst layers before downward percolation of water was observed. There can be delays of up to several months since the rain season began owing to the time it takes to saturate the soil which becomes dry each summer

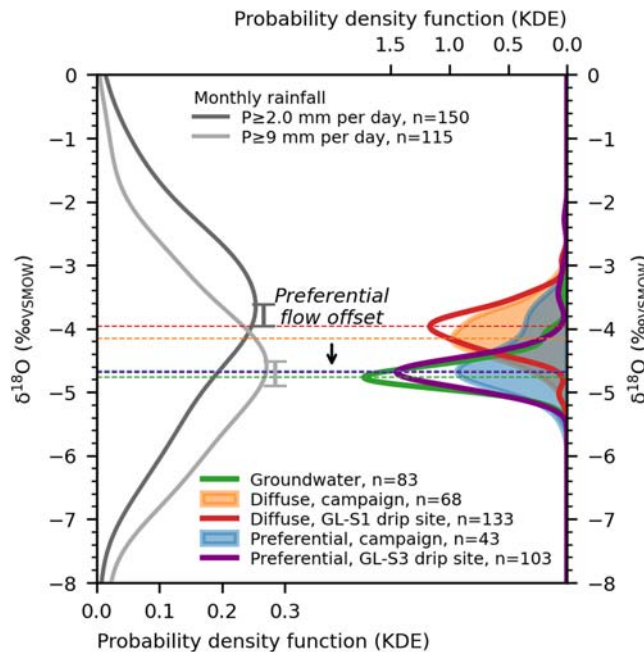


Fig. 5 Distributions of $\delta^{18}\text{O}$ values for Calgardup rainfall, Golgotha drip water and groundwater. Drip waters with a greater preferential-flow influence are ^{18}O -depleted with respect to diffuse flow and indicate a recharge bias. For drip water, both the campaign dataset (~20 drip sites) and the long-term sampling (two drip sites: GL-S1 and GL-S3) are shown. The distribution of preferential-flow drip waters (blue/purple) are shifted to lower $\delta^{18}\text{O}$ values compared with the distribution for diffuse-flow drips (orange/red). Preferential flow and groundwater $\delta^{18}\text{O}$ (green) values closely agree indicating that infiltration to groundwater similarly has a recharge bias towards higher-intensity rainfall. Groundwater data are Holocene age data for the Southern Perth Basin (Leederville and Yarragadee aquifers) taken from ref. 58. Dashed lines indicate the distribution modes (values given in text). Precipitation-weighted monthly rain $\delta^{18}\text{O}$ values were used for comparing with drip waters to approximate the sampling interval of the drip waters (4–6 weeks). Error bars show the mean ± 2 standard deviation of the precipitation-weighted monthly rain $\delta^{18}\text{O}$ values. We expect that the distribution of drip water to be narrower since drip water is the averaging of rain events. The gaussian_KDE routine from scipy Python library was used for computing kernel density estimates. This employs a Gaussian kernel, with a bandwidth computed using the method from ref. 59.

(see Supplementary Note 1 for further description). As seasonal saturation of the soil and epikarst zone is needed to initiate recharge of karst stores above the monitored drip sites, it follows that the opportunity for recharge each season will also depend on the number of days that the soil remains saturated each season³⁹.

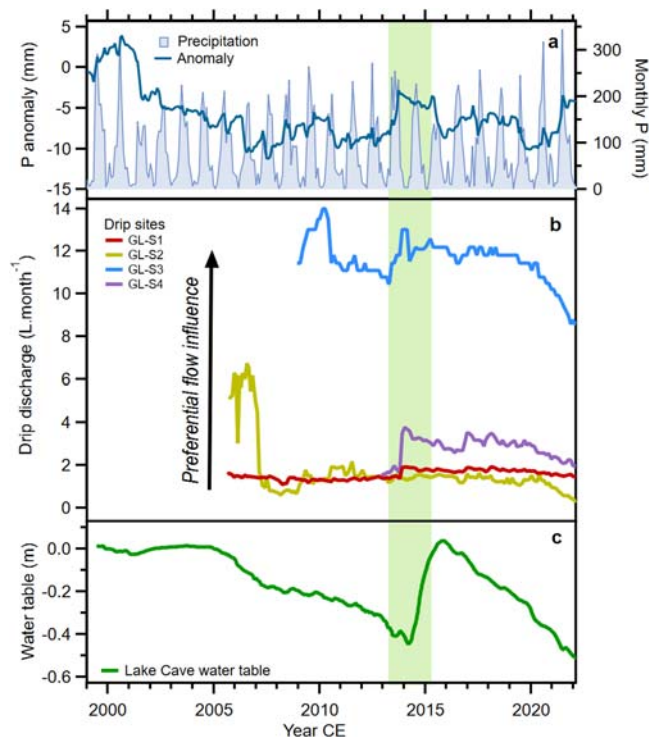


Fig. 6 Rainfall recharge and the response of drip discharge and the local water table. Higher rainfall (e.g., green bar) increases flow along preferential-flow pathways and recharge to the local water table. **a** Monthly meteoric precipitation and their smoothed anomalies. **b** Drip discharge from four speleothem sites in this study. **c** Water table data beneath Lake Cave, 3.6 km from Golgotha Cave. Precipitation and drip discharge data are for Golgotha Cave. Drip discharge data were calculated using drip rates from the long-term monitored sites and assuming a drip volume of 0.1433 ml (as in ref. ¹²) and an average of 30.4 days per month. Monthly precipitation anomalies were calculated using the climatological means from 1950 to 2020 and applying an exponentially weighted moving average with a half-life parameter of 36.6 months. Water table level data are relative to the first measurement (June 1999).

We examined temporal variability in the frequency of days that the soil moisture was saturated by extracting modelled soil moisture values for the four cave sites for 1911–2019 from the Australian Bureau of Meteorology’s Australian Water Resources Assessment Landscape model³³ (see ‘Methods’). Prior to the first rainfall decrease, the average seasonal duration of soil saturation was 96 days per year (1910–1968; Fig. 3d). This decreased to 66 days per year (1969–1999) following the first rainfall decrease and to 55 days per year (1999–2020) after the second rainfall decrease (Fig. 3d). This represents an overall drop of 43% in the number of days that the soil is saturated.

As stated above, a reduction in the duration of the soil saturation will reduce the potential contribution of recharge from preferential flow, and consequently impact the $\delta^{18}\text{O}$ values of the drip water. Our analysis of the modelled soil moisture data suggests that this seasonal window in which recharge from preferential flow is possible has almost halved since regional rainfall began declining. The shrinking of this seasonal window coincides with the period of the $\delta^{18}\text{O}$ uptick (Fig. 3a, d) with the uptick accelerating in the last two decades (Fig. 3a). Thus, it appears that the majority of the isotopic uptick is in response to the second rather than the first rainfall decrease. This likely reflects the cumulative impact of reduced rainfall on soil moisture, whereby reduced saturation in the soil profile and the reduction in the duration when the soil/epikarst is recharging the

karst stores, reduces the likelihood of preferential flow along fractures or conduits occurring. That is, we propose that preferential flow is still occurring but was reduced during the period of the first rainfall decrease (1969–1999), and was further reduced when the second rainfall decrease occurred after 1999. A further consideration is the lag for karst stores to drain. For example, the fracture activation event observed for GL-S4 drip water (described above and see ref. ²⁷) took at least 3 years for drip water $\delta^{18}\text{O}$ to return to values equivalent to diffuse-flow drips²⁷. Thus we interpret that the impact of a reduced water balance has decreased recharge along preferential-flow paths in the karst, resulting in the uptick in drip water and hence speleothem $\delta^{18}\text{O}$ values.

Implications for understanding rainfall recharge to ground-water. Preferential-flow paths with their higher drip rates will contribute more rainfall recharge to groundwater volumetrically. This is supported by ref. ¹²: the estimated total flux from the ceiling area of Golgotha Cave with a higher proportion of drips fed by preferential flow was 39% higher compared with the ceiling area predominately supplied by the diffuse flow. This is also supported by water table measurements at Lake Cave (2000–2022; Fig. 1 for location) overlapping the period of drip discharge monitoring (2005–2022; Golgotha Cave) in Fig. 6. For example, higher rainfall in 2013 (Fig. 6a) resulted in a rapid rise in discharge for drips with a greater preferential-flow influence (Fig. 6b) and this coincided with the local water table also rising approximately 0.5 m (Fig. 6c). In comparison, the discharge from diffuse-flow dominated drips showed little to no response (Fig. 6b). We also compared the isotopic value of drip water and groundwater, and this further supports that rainfall recharge to groundwater beneath these caves occurs primarily via preferential flow. i.e., Fig. 5 shows that the distribution mode of preferential-flow-influenced drip water $\delta^{18}\text{O}$ values ($-4.67 \pm 0.06\text{‰}_{\text{VMSOW}}$; campaign data) closely agrees with that of Holocene groundwater $\delta^{18}\text{O}$ values (mode: $-4.67 \pm 0.03\text{‰}$).

A reduction in preferential flow will also lead to a volumetric decline in rainfall recharge to groundwater. This is observed in a dataset of longer water table observations from another cave system in the region (Jewel Cave, Fig. 1 for location) that spans the period of the rainfall decrease (Fig. 3e). This record began in the 1950s and confirms a decline in the volume of rainfall recharge to the local water table that began around 1980 (Fig. 3e), in agreement with the beginning of the $\delta^{18}\text{O}$ uptick. This volumetric decline in rainfall recharge to groundwater, as well as drier catchments with reduced runoff and fewer major flooding events have also been recorded in the Perth Basin and throughout southwest Australia^{22,42}.

Rainfall recharge in the paleo record. Our study offers a well-constrained processed-based relationship between rising speleothem $\delta^{18}\text{O}$ values in response to a sustained decrease in rainfall. Importantly, it has been shown that the uptick in $\delta^{18}\text{O}$ was in response to a reduction in the preferential-flow component to drip waters that is likely linked to the seasonal duration of soil moisture, rather than a shift in mean annual rainfall $\delta^{18}\text{O}$ values. The large magnitude of the $\delta^{18}\text{O}$ uptick highlights that this mechanism amplifies the response of the speleothem $\delta^{18}\text{O}$ signal to hydrological forcing. Thus, the identification of replicated upticks in speleothems can be used to identify past reductions in rainfall recharge to groundwater in a region.

The speleothem record from Golgotha Cave²⁷ provides a multi-century context to assess the recent $\delta^{18}\text{O}$ uptick. Stalagmite GL-S4 grew continuously since 1200 CE with a robust chronology constructed from annual laminae counting (Fig. 7a). It was

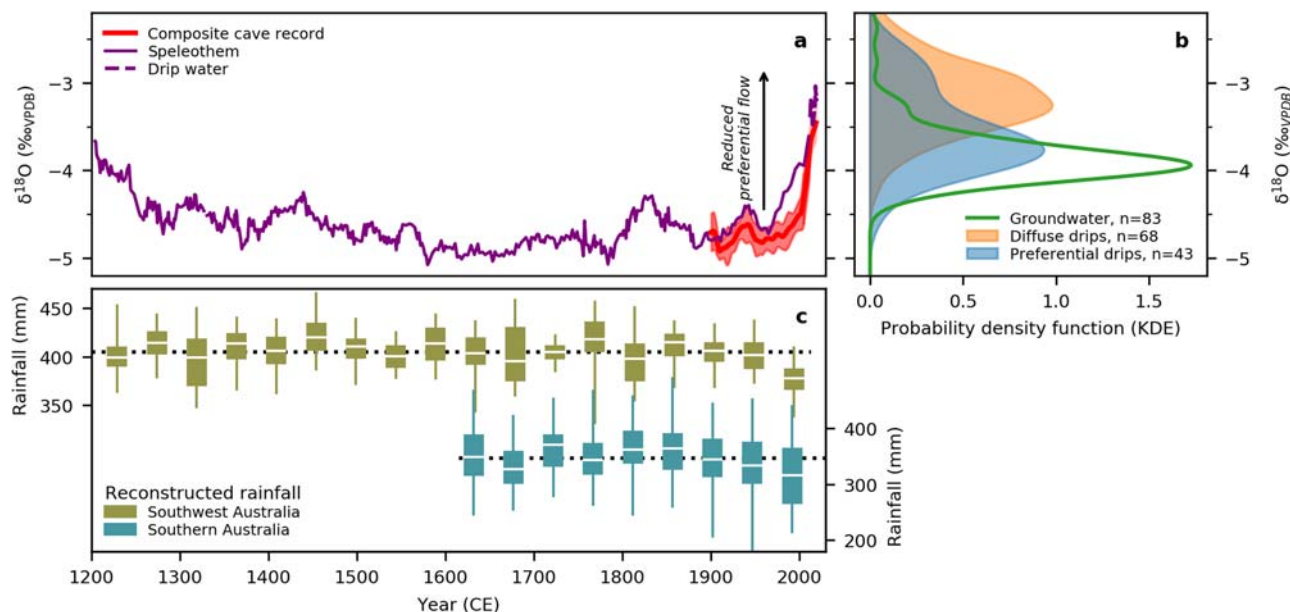


Fig. 7 Recent uptick in $\delta^{18}\text{O}$ values indicates a disconnection in rainfall recharge (reduced preferential flow) to groundwater that is unprecedented in the last 800 years. Cave record compared with reconstructed annual rainfall for southwest Australia^{43,60} and southern Australia⁴⁴. **a** Golgotha Cave $\delta^{18}\text{O}$ record: speleothem GL-S4²⁷ (solid purple) plus drip water (dashed purple) and composite record (red). **b** Distributions of drip water and Holocene groundwater $\delta^{18}\text{O}$ values on the calcite-equivalent (VPDB) scale for comparison with the speleothem record. **c** Southwest Australian precipitation (olive) reconstructed from snow accumulation rates at Law Dome, Antarctica, where higher ice accumulation is related to reduced rainfall in southwest Australia^{43,60} and southern Australian precipitation (teal) reconstructed from multiple paleoclimate proxies⁴⁴. Rainfall reconstructions are shown as box and whisker plots with long-term mean values shown as dotted lines, grouped into 45-year bins, whiskers show min/max and boxes show 25/50/75th percentiles. Reference⁶⁰ identified 1971 as a statistically significant change in the Law Dome-based rainfall reconstruction.

identified as fed by diffuse drip water supplied from the matrix but also by preferential flow along fractures that activate during wetter years²⁷. The other three speleothems were supplied either predominately by diffuse flow (GL-S1) or by complex fractures (GL-S2 and GL-S3). Thus GL-S4 is the most suitable record to assess variability in preferential-flow contribution in the longer-term context. Speleothem $\delta^{18}\text{O}$ values for GL-S4 are approximately $-3.9\text{‰}_{\text{VPDB}}$ or lower, consistent with preferential flow along a feeding fracture contributing to the drip water for the record from around 1200 CE until the late-1990s CE, when the trend to higher values indicates that the contribution of preferential flow has rapidly decreased and that the drip water has become predominately supplied by diffuse flow (Fig. 7a, b). The modal value for groundwater on the calcite-equivalent scale is $-3.9\text{‰}_{\text{VPDB}}$, and is also compared with the longer speleothem record on Fig. 7a, b. This study has linked recharge to the caves along preferential flow paths to rainfall recharge of regional groundwater, both isotopically (Fig. 5) and volumetrically (Fig. 6). Thus the longer GL-S4 speleothem record presented here implies that the southwest Australian region is currently experiencing a reduction in rainfall recharge to groundwater that is unprecedented for the last eight centuries.

Our cave-based reconstruction builds on evidence for the hydroclimate history of southwest Australia from other paleoclimate archives. Figure 7a, c compares the speleothem GL-S4 rainfall recharge $\delta^{18}\text{O}$ record with two reconstructions of rainfall for southwest Australia based on: (1) the Law Dome ice core record from Antarctica^{17,43} and (2) multiple paleoclimate records from the wider southern Australian region^{44,45} (see Fig. 1 for locations). The recent rainfall decrease is highlighted as particularly dry in these longer reconstructions with the ice core-based reconstruction indicating that the decrease in rainfall is also unprecedented for the last eight centuries. Our study presented here confirms this interpretation with evidence directly from the southwest Australian

region rather than distal reconstructions based on atmospheric teleconnections. Importantly, the cave study demonstrates that the impact of the rainfall decline has resulted in an unprecedented decrease in rainfall recharge to groundwater for the last eight centuries. The chronology for the Law Dome-based rainfall reconstruction for southwest Australia is longer than that for GL-S4 and suggests two possible earlier intervals of comparable rainfall decrease during 385–429 CE and 732–776 CE. Extending the southwest Australian speleothem record in future studies will assist in understanding whether comparable dry periods that are persistent enough to impact rainfall recharge exist in the local record. Additionally, tree-ring records from Lake Deborah⁴⁵ identify evidence for two prolonged droughts in around 1755–1785 CE and 1828–1859. While these may have been of insufficient duration and/or intensity to drive sustained reductions in preferential flow and disconnection to groundwater, the speleothem record does display relatively higher $\delta^{18}\text{O}$ values in these two periods, particularly the early-mid-1800s, lending support to a reduction in rainfall recharge to Golgotha Cave at these times also. In addition, the tree-ring records should reflect greater hydroclimate sensitivity as these records are located in more arid inland areas (Fig. 1), compared to the relatively wet coastal fringe for our cave sites.

Conclusions. In this study, the $\delta^{18}\text{O}$ of drip waters and calcite deposited from them in caves located in the vadose zone, and where recharge can be identified unambiguously as being from rainfall, have provided clear evidence of decreased rainfall recharge to groundwater resources. We confirm that no replicated uptick events are seen in the last 800 years in the stalagmite record from the southwest Australian region²⁷ suggesting that the current decoupling of rainfall to groundwater recharge is unprecedented for the last eight centuries. This has important

implications for contextualising the threat to the biodiversity in groundwater-dependent ecosystems and sustainable use of groundwater in a region heavily dependent on it for agriculture, and where future use is anticipated to increase²². The recent speleothem and drip water dataset indicates that rainfall recharge to groundwater may no longer be reliably occurring and highlights the immediate threat of climate change to water security in a region heavily dependent on groundwater.

Our findings are relevant for future climate change also as there is debate over the modelled changes in rainfall intensity and whether that would amplify hydrological responses. Runoff (i.e., flooding) has been the focus of research and adaptation planning so far⁴⁶, with little attention until now given to the implications of future climate change on groundwater recharge. This study shows that a network of monitored caves in other regions where groundwater is relied upon could serve as a direct and unambiguous measurement of reduced recharge, particularly in karstified carbonate rocks that have flow paths associated with both primary porosity and fractures (e.g., as also observed in an Ethiopian stalagmite⁴⁷) and widespread rainfall declines are expected this century as a result of human-caused climate change⁴⁸. Monitoring also provides valuable data for ground-truthing speleothem paleoclimate records, while upticks in the speleothem paleoclimate records provide a longer-term context for evaluating if current groundwater recharge changes are outside the range of natural variability, thus the risks to groundwater resources from natural and human-caused climate changes.

Methods

Speleothem chronologies. Chronologies for all speleothems were published previously. Briefly, all stalagmites had been actively forming at the time that they were removed from the caves and the date of removal from the cave is used as the youngest age. The chronologies for CRY-S1⁴⁹, GL-S3 and GL-S4²⁷ were determined from annual laminae counting of 2D maps of Sr concentration; MND-S1 from annual laminae counting of Ba concentration from duplicate transects⁵⁰; LAB-S1 from the peak fitting method of ref. ⁵¹ utilising principal components analysis of duplicate transects of Ba, Sr and U concentrations; while GL-S1 and GL-S2 chronologies were determined from bomb pulse detection using radiocarbon analyses⁵² and U/Th disequilibrium dating²⁷. Mean annual extension rates for CRY-S1, GL-S4 and LAB-S1 through time were compared by calculating the mean and standard deviation of annual laminae width for each decade.

Speleothem $\delta^{18}\text{O}$. Data were previously published for all records^{27,30,53} with the exception of CRY-S1 and LAB-S1. Milling and isotope ratio mass spectrometry methods are as described in ref. ²⁷. CRY-S1 $\delta^{18}\text{O}$ measurements were made at the Mark Wainwright Analytical Centre at UNSW Sydney using a MAT-253 isotope ratio mass spectrometer with Kiel carbonate device (25–50 μg samples). LAB-S1 $\delta^{18}\text{O}$ measurements were made at the Research School of Earth Sciences, ANU, using a Thermo MAT-253 isotope ratio mass spectrometer coupled to a Kiel IV carbonate device (110–130 μg samples). Data in both laboratories are normalised to the Vienna Pee Dee Belemnite (VPDB) scale using NBS19 ($\delta^{18}\text{O} = -2.20\text{‰}$ and $\delta^{13}\text{C} = +1.95\text{‰}$) and NBS-18 ($\delta^{18}\text{O} = -23.0\text{‰}$ and $\delta^{13}\text{C} = -5.0\text{‰}$).

Golgotha Cave drip water and farmed calcite $\delta^{18}\text{O}$. Drip water data, sampled at 4–6 weekly intervals; and farmed calcites, in situ for 9–31 months, were previously published in ref. ²⁷. Data and methods for converting drip waters from the VSMOW scale to a calcite equivalent on the VPDB scale were also previously published²⁷ using mean annual cave temperature measured at Golgotha Cave ($14.6 \pm 0.1\text{ }^\circ\text{C}$) and the bulk empirical fractionation factor for Golgotha Cave (1.0318 ± 0.0004) determined therein.

Composite speleothem record. Speleothem, and drip water $\delta^{18}\text{O}$ data (as calcite-equivalent values) were interpolated to be annually resolved to construct the composite record. For Golgotha Cave speleothem records this represented a 3–5 \times increase in resolution, and for records CRY-S1 and LAB-S1, this represented a 2–3 \times decrease in resolution relative to the original data. Alternative methods were investigated such as maintaining the sampled resolution and weighting each data point according to the time interval that it represents, and the uptick in $\delta^{18}\text{O}$ values is still robust i.e., the choice of method for compositing the data did not affect the interpretation. We considered uncertainty in the age-depth models but this is least at the youngest end, i.e., 0% at the year of collection and still small at 1900 CE (range: ± 2 to 18%, 2σ). It was not necessary to account for analytical uncertainty in $\delta^{18}\text{O}$ as these are small (0.05‰ for carbonates and 0.1‰ for water)²⁷.

Rainfall $\delta^{18}\text{O}$ data. Annual rainfall amount for southwest Australia (line joining 30°S, 115°E and 35°S, 120°E; Fig. 1, inset) and the extent of the Tamala Limestone (Fig. 1) was extracted from Bureau of Meteorology gridded spatial data³³. Annual and monthly amount-weighted $\delta^{18}\text{O}$ was measured at the Perth Global Network of Isotopes in Precipitation (GNIP) site⁵⁴ and Calgardup²⁶. Predicted amount-weighted annual $\delta^{18}\text{O}$ were calculated from an empirical relationship between daily $\delta^{18}\text{O}$ and daily precipitation, Eq. (3) in ref. ²⁶, applied to Bureau of Meteorology rainfall observations from the high quality⁵⁵ sites Boyanup and Cape Naturaliste.

Soil moisture data. Modelled soil moisture data were extracted for each cave site from the Australian Bureau of Meteorology's Australian Water Resources Assessment Landscape model: AWRA-L version 6⁵⁶. Briefly, AWRA-L is a continent-wide water balance model with 0.05° gridded outputs of soil moisture, runoff, evapotranspiration and drainage. We utilised daily soil moisture in the lower (0.1–1 m; term Ss) and deep soil store (1–6 m; term Sd), as well as rainfall (term P_g) and actual evapotranspiration (term E_{tot})⁵⁶. Model output (Ss), validated against field measurements of soil moisture at Golgotha Cave³⁸ (see Supplementary Fig. 2) and the Sd output, corresponding to the observed depth of seasonal wetting prior to initiation of percolation into the host rock³⁹ is used to calculate the number of days per year when soil is saturated. The best match between observed and modelled soil moisture data is 66%; however, observed recharge at Golgotha suggests a higher percentile (78th) would be representative of fracture activation necessary for recharge, and we apply this to all five sites. See Supplementary Fig. 2 for further details.

Data availability

The Golgotha speleothem and drip water time series data may be found on the PANGEA paleoclimate data repository (PDI-30276 and PDI-30277). The authors have submitted all speleothem data to database version 3 of SISAL (Speleothem Isotope Synthesis and AnaLysis; a PAGES-funded Working Group). Weather station and gridded climate data are available from the Australian Bureau of Meteorology, <http://www.bom.gov.au>.

Received: 2 May 2022; Accepted: 19 May 2023;

Published online: 09 June 2023

References

- Cuthbert, M. O. et al. Observed controls on resilience of groundwater to climate variability in sub-Saharan Africa. *Nature* **572**, 230–234 (2019).
- Jasechko, S. et al. Global aquifers dominated by fossil groundwaters but wells vulnerable to modern contamination. *Nat. Geosci.* **10**, 425 (2017).
- Hughes, C. E., Cendón, D. I., Johansen, M. P. & Meredith, K. T. Climate change and groundwater. In *Sustaining Groundwater Resources* (ed. Jones, J. A. A.), 97–117 (Springer, 2011).
- Cuthbert, M. O. et al. Global patterns and dynamics of climate–groundwater interactions. *Nat. Clim. Chang.* **9**, 137–141 (2019).
- Dragoni, W. & Sukhija, B. S. *Climate Change and Groundwater* (Geological Society, 2008).
- Kløve, B. et al. Climate change impacts on groundwater and dependent ecosystems. *J. Hydrol.* **518**, 250–266 (2014).
- Hughes, J. D., Petrone, K. C. & Silberstein, R. P. Drought, groundwater storage and stream flow decline in southwestern Australia. *Geophys. Res. Lett.* **39**, (2012).
- Taylor, R. G. et al. Ground water and climate change. *Nat. Clim. Chang.* **3**, 322 (2012).
- Herrera-Pantoja, M. & Hiscock, K. M. The effects of climate change on potential groundwater recharge in Great Britain. *Hydrol. Process.* **22**, 73–86 (2008).
- Cochand, F., Brunner, P., Hunkeler, D., Rössler, O. & Holzkämper, A. Cross-sphere modelling to evaluate impacts of climate and land management changes on groundwater resources. *Sci. Total Environ.* **798**, 148759 (2021).
- Wöhling, T., Wilson, S., Wadsworth, V. & Davidson, P. Detecting the cause of change using uncertain data: Natural and anthropogenic factors contributing to declining groundwater levels and flows of the Wairau Plain aquifer, New Zealand. *J. Hydrol.: Regional Stud.* **31**, 100715 (2020).
- Mahmud, K. et al. Estimation of deep infiltration in unsaturated limestone environments using cave lidar and drip count data. *Hydrol. Earth Syst. Sci.* **20**, 359–373 (2016).
- Beal, L. K. et al. Isotopic and geochemical assessment of the sensitivity of groundwater resources of Guam, Mariana Islands, to intra- and inter-annual variations in hydroclimate. *J. Hydrol.* **568**, 174–183 (2019).
- Jukić, D. & Denić-Jukić, V. Groundwater balance estimation in karst by using a conceptual rainfall-runoff model. *J. Hydrol.* **373**, 302–315 (2009).
- Baker, A. et al. Global analysis reveals climatic controls on the oxygen isotope composition of cave drip water. *Nat. Commun.* **10**, 2984 (2019).

16. Vogel, J. C. & Van Urk, H. Isotopic composition of groundwater in semi-arid regions of southern Africa. *J. Hydrol.* **25**, 23–36 (1975).
17. Zheng, Y. et al. Extending and understanding the South West Western Australian rainfall record using a snowfall reconstruction from Law Dome, East Antarctica. *Clim. Past Discuss.* **2020**, 1–32 (2020).
18. Delworth, T. L. & Zeng, F. Regional rainfall decline in Australia attributed to anthropogenic greenhouse gases and ozone levels. *Nat. Geosci.* **7**, 583–587 (2014).
19. Hope, P., Timbal, B. & Fawcett, R. Associations between rainfall variability in the southwest and southeast of Australia and their evolution through time. *Int. J. Climatol.* **30**, 1360–1371 (2010).
20. Bryan, E., Meredith, K. T., Baker, A., Post, V. E. A. & Andersen, M. S. Island groundwater resources, impacts of abstraction and a drying climate: Rottneest Island, Western Australia. *J. Hydrol.* **542**, 704–718 (2016).
21. Ali, R. et al. Potential climate change impacts on groundwater resources of south-western Australia. *J. Hydrol.* **475**, 456–472 (2012).
22. McFarlane, D. et al. Climate change impacts on water yields and demands in south-western Australia. *J. Hydrol.* **475**, 488–498 (2012).
23. Barron, O. et al. Projected risks to groundwater-dependent terrestrial vegetation caused by changing climate and groundwater abstraction in the Central Perth Basin, Western Australia. *Hydrol. Process.* **28**, 5513–5529 (2014).
24. Barron, O. et al. Climate change effects on water-dependent ecosystems in south-western Australia. *J. Hydrol.* **434–435**, 95–109 (2012).
25. Lipar, M. & Webb, J. A. Middle-late Pleistocene and Holocene chronostratigraphy and climate history of the Tamala Limestone, Cooloongup and Safety Bay Sands, Nambung National Park, southwestern Western Australia. *Aust. J. Earth Sci.* **61**, 1023–1039 (2014).
26. Griffiths, A. D., Treble, P., Hope, P. & Rudeva, I. Rainfall stable water isotope variability in coastal southwestern Western Australia and its relationship to climate on multiple timescales. *J. Geophys. Res. Atmos.* **127**, 31 (2022).
27. Treble, P. C. et al. Ubiquitous karst hydrological control on speleothem oxygen isotope variability in a global study. *Commun. Earth Environ.* **3**, 29 (2022).
28. Mahmud, K., Mariethoz, G., Baker, A. & Treble, P. C. Hydrological characterization of cave drip waters in a porous limestone: Golgotha Cave, Western Australia. *Hydrol. Earth Syst. Sci.* **22**, 977–988 (2018).
29. Mahmud, K., Mariethoz, G., Treble, P. C. & Baker, A. Terrestrial LiDAR survey and morphological analysis to identify infiltration properties in the Tamala Limestone, Western Australia. *IEEE J. Sel. Top. Appl. Earth Obs. Remote Sens.* **8**, 4871–4881 (2015).
30. Treble, P. et al. In situ measurement of seasonal $\delta^{18}\text{O}$ variations and analysis of isotopic trends in a modern speleothem from southwest Australia. *Earth Planet Sci. Lett.* **233**, 17–32 (2005).
31. Lachniet, M. S. Climatic and environmental controls on speleothem oxygen-isotope values. *Quat. Sci. Rev.* **28**, 412–432 (2009).
32. Fairchild, I. J. et al. Modification and preservation of environmental signals in speleothems. *Earth-Sci. Rev.* **75**, 105–153 (2006).
33. Bureau of Meteorology. Climate Data Online. 2020 [cited 2020 August 2020]. <http://www.bom.gov.au/climate/change/index.shtml#tabs=Tracker> (2020).
34. Deininger, M. et al. Are oxygen isotope fractionation factors between calcite and water derived from speleothems systematically biased due to prior calcite precipitation (PCP)? *Geochim. Cosmochim. Acta* **305**, 212–227 (2021).
35. Day, C. C. & Henderson, G. M. Oxygen isotopes in calcite grown under cave-analogue conditions. *Geochim. Cosmochim. Acta* **75**, 3956–3972 (2011).
36. Philip, P. & Yu, B. Interannual variations in rainfall of different intensities in South West of Western Australia. *Int. J. Climatol.* **40**, 3052–3071 (2020).
37. Cuthbert, M. O. et al. Drip water isotopes in semi-arid karst: Implications for speleothem paleoclimatology. *Earth Planet Sci. Lett.* **395**, 194–204 (2014).
38. Treble, P. C. et al. An isotopic and modelling study of flow paths and storage in Quaternary calcarenite, SW Australia: implications for speleothem paleoclimate records. *Quat. Sci. Rev.* **64**, 90–103 (2013).
39. Leopold, M., Gupanis-Broadway, C., Baker, A., Hankin, S. & Treble, P. Time lapse electric resistivity tomography to portray infiltration and hydrologic flow paths from surface to cave. *J. Hydrol.* **593**, 125810 (2021).
40. Yakir, D. & Wang, X.-F. Fluxes of CO_2 and water between terrestrial vegetation and the atmosphere estimated from isotope measurements. *Nature* **380**, 515–517 (1996).
41. Ireson, A. M., Butler, A. B. & Wheeler, H. S. Evidence for the onset and persistence with depth of preferential flow in unsaturated fractured porous media. *Hydrol. Res.* **43**, 707–719 (2012).
42. McFarlane, D., George, R., Ruprecht, J., Charles, S. & Hodgson, G. Runoff and groundwater responses to climate change in South West Australia. *J. Royal Soc. West. Aust.* **103**, 9–27 (2020).
43. van Ommen, T. D. & Morgan, V. Snowfall increase in coastal East Antarctica linked with southwest Western Australian drought. *Nat. Geosci.* **3**, 267 (2010).
44. Freund, M., Henley, B. J., Karoly, D. J., Allen, K. J. & Baker, P. J. Multi-century cool- and warm-season rainfall reconstructions for Australia's major climatic regions. *Clim. Past* **13**, 1751–1770 (2017).
45. O'Donnell, A. J., McCaw, W. L., Cook, E. R. & Grierson, P. F. Megadroughts and pluvials in southwest Australia: 1350–2017 CE. *Clim. Dynam.* **57**, 1817–1831 (2021).
46. Fowler, H. J., Wasko, C. & Prein, A. F. Intensification of short-duration rainfall extremes and implications for flood risk: current state of the art and future directions. *Philos. Transact. Royal Soc. A: Math. Phys. Eng. Sci.* **379**, 20190541 (2021).
47. Asrat, A. et al. A high-resolution multi-proxy stalagmite record from Mechara, Southeastern Ethiopia: palaeohydrological implications for speleothem palaeoclimate reconstruction. *J. Quat. Sci.* **22**, 53–63 (2007).
48. IPCC. *Climate Change 2021: The Physical Science Basis. Contribution of Working Group I to the Sixth Assessment Report of the Intergovernmental Panel on Climate Change.* (eds Masson-Delmotte, V. et al.) 2391 (Cambridge University Press, 2021).
49. Baker, A. et al. The properties of annually laminated stalagmites—a global synthesis. *Rev. Geophys.* **59**, e2020RG000722 (2021).
50. Treble, P., Shelley, J. M. G. & Chappell, J. Comparison of high resolution sub-annual records of trace elements in a modern (1911–1992) speleothem with instrumental climate data from southwest Australia. *Earth Planet Sci. Lett.* **216**, 141–153 (2003).
51. Nagra, G. et al. Dating stalagmites in Mediterranean climates using annual trace element cycles. *Sci. Rep.* **7**, 621 (2017).
52. Markowska, M. et al. Modelling the ^{14}C bomb-pulse in young speleothems using a soil carbon continuum model. *Geochim. Cosmochim. Acta* **261**, 342–367 (2019).
53. McDonough, L. et al. Past fires and post-fire impacts reconstructed from a southwest Australian stalagmite. *Geochimica et Cosmochimica Acta* **325**, 258–277 (2022).
54. Hollins, S. E., Hughes, C. E., Crawford, J., Cendón, D. I. & Meredith, K. T. Rainfall isotope variations over the Australian continent—implications for hydrology and isoscape applications. *Sci. Total Environ.* **645**, 630–645 (2018).
55. Lavery, B., Joung, G. & Nicholls, N. An extended high-quality historical rainfall dataset for Australia. *Australian Meteorological Magazine* **46**, 27–38 (1997).
56. Frost, A. J., Ramchurn, A. & Smith, A. The Australian Landscape Water Balance model (AWRA-L v6). *Technical Description of the Australian Water Resources Assessment Landscape model version 6.* (Bureau of Meteorology Technical Report, 2018).
57. Yoshimura, K., Kanamitsu, M., Noone, D. & Oki, T. Historical isotope simulation using Reanalysis atmospheric data. *J. Geophys. Res. Atmos.* **113**, (2008).
58. Priestley, S. C. et al. A 35 ka record of groundwater recharge in south-west Australia using stable water isotopes. *Sci. Total Environ.* **717**, 135105 (2020).
59. Scott, D. W. *Multivariate Density Estimation: Theory, Practice and Visualization* (John Wiley & Sons, Inc, 1992).
60. Zheng, Y. et al. Extending and understanding the South West Western Australian rainfall record using a snowfall reconstruction from Law Dome, East Antarctica. *Clim. Past* **17**, 1973–1987 (2021).

Acknowledgements

This research is supported by funding from the Australian Research Council (DP140102059 to PCT and NJA). The Sr map used for CRY-S1 chronology was obtained on the X-ray fluorescence microscopy (XFM) beamline at the Australian Synchrotron, part of ANSTO under proposals PA14312. The authors would like to thank Carolina Paice (Parks and Wildlife Services at Leeuwin-Naturaliste National Park) and Mark Delane (Margaret River Busselton Tourism Association) for providing cave water level data and reports. We also thank Carolina and staff at Calgardup Caves for their dedication in maintaining the long-term monitoring of drip water in Golgotha Cave. We would also like to thank Nevena Kosarac and Liza McDonough for assistance with laminae counting of CRY-S1, and Lewis Adler and Mark Wainwright for IRMS analytical support. This research was undertaken with the assistance of resources and services from the National Computational Infrastructure (NCI), which is supported by the Australian Government. IsoGSM data which appears in this article, was provided thanks to Kei Yoshimura. The authors respectfully acknowledge the Wadandi Noongar peoples as the traditional and spiritual custodians of the study region.

Author contributions

This manuscript was devised by P.C.T., A.B. and S.C.P. S.C.P., P.C.T. and A.D.G. collated the data and prepared the figures. P.C.T., N.J.A. and K.T.M. conducted analyses and provided data. S.C.P. wrote the manuscript with input from all co-authors.

Competing interests

The authors declare no competing interests.

Additional information

Supplementary information The online version contains supplementary material available at <https://doi.org/10.1038/s43247-023-00858-7>.

Correspondence and requests for materials should be addressed to Stacey C. Priestley.

Peer review information *Communications Earth & Environment* thanks Weimin Feng and the other, anonymous, reviewer(s) for their contribution to the peer review of this work. Primary Handling Editors: Olga Churakova and Joe Aslin. A peer review file is available.

Reprints and permission information is available at <http://www.nature.com/reprints>

Publisher's note Springer Nature remains neutral with regard to jurisdictional claims in published maps and institutional affiliations.



Open Access This article is licensed under a Creative Commons Attribution 4.0 International License, which permits use, sharing, adaptation, distribution and reproduction in any medium or format, as long as you give appropriate credit to the original author(s) and the source, provide a link to the Creative Commons license, and indicate if changes were made. The images or other third party material in this article are included in the article's Creative Commons license, unless indicated otherwise in a credit line to the material. If material is not included in the article's Creative Commons license and your intended use is not permitted by statutory regulation or exceeds the permitted use, you will need to obtain permission directly from the copyright holder. To view a copy of this license, visit <http://creativecommons.org/licenses/by/4.0/>.

© Crown 2023